Characterization of Microwave Properties of Superconducting NbTiN Films Using TDS

Fedor V. Khan, Elena S. Zhukova, Boris P. Gorshunov, Lenar S. Kadyrov, Artem M. Chekushkin, Andrey V. Khudchenko, and Valery P. Koshelets, *Member, IEEE*

***Abstract*—In this article, we perform systematic study of electrodynamic properties of superconducting NbTiN films at frequencies 0.2–2.5 terahertz (THz) and in temperature range from 4 to 15 K using time-domain spectrometer. The goal is to achieve the best parameters of the films at THz frequencies; that is to reach a tradeoff between the highest possible normal state conductivity σ_0, the smallest London penetration depth λ_L, and the highest energy gap and critical temperature T_c. To do this, it is necessary to determine the optimal manufacturing conditions; to this end, a set of NbTiN films of various compositions was fabricated, controlled by the nitrogen pressure in the magnetron chamber. As a result, the film with parameters $\sigma_0 = 11{\cdot}10^3$ 1/(Ohm·cm), $\lambda_L = 280$ nm, and $T_c = 14.4$ K were obtained. To fit the experimental data, two models with and without taking intragap states into account were used, and both of them are in good agreement with experiment.**

***Index Terms*—Intragap states, strong-coupling superconductors, superconducting materials, terahertz (THz) measurements, thin films, time-domain spectroscopy.**

I. Introduction

SUPERCONDUCTING electronics play significant role in novel fundamental research [1], ground-based [2], [3] and space-based [4], [5] radio astronomy, spectroscopy [6], [7], biology [8], single photon detectors [9], and quantum systems [10]. Heterodyne receivers based on superconductor–insulator–superconductor tunnel junctions have noise temperature approaching quantum limit [11], [12] and operate at terahertz (THz) and sub-THz frequencies, which make them invaluable for ultrasensitive measurements in this range. New advances in development of superconducting devices can be achieved by optimizing production processes and implementing new materials. In particular, the use of niobium compounds (e.g., NbN and NbTiN) enables one to broaden the operating range of the devices up to 1.2 THz.

Studies of the films made of NbN and NbTiN were performed by a number of groups around the world and various methods have been proposed. In works by Uzawa et al. [13] and [14], the authors fabricated films using magnetron sputtering and characterized them by transmission with a time-domain spectrometer (TDS). The thicknesses of the films in those works were about 150 and 50 nm, which are much less than the typical thickness of the electrodes of superconducting transmission lines which should be equal to or larger than London penetration depth (280 nm or even larger for NbTiN films at temperatures far below T_c measured at frequencies less than 0.1 THz, that is much less than the gap frequency). In [15], the authors optimized their fabrication process in order to achieve the lowest possible London penetration depth and increase T_c. The parallel plate resonator technique [16] was used to study the films at frequencies around 20 GHz. However, the parameters of the superconducting films at high frequencies, especially close to the gap frequency, are different from those obtained by dc measurements.

Therefore, in this article, we continue our previous article [17] and study a series of superconducting NbTiN films with thicknesses of about 330 nm, which is the typical thickness of the electrodes in real superconducting devices operating at THz frequencies.

The rest of the article is organized as follows. The fabrication processes of the films are described in Section II. Section III is devoted to the experimental setup and the model used to fit the experimental data. Further discussion on models of strongly coupled superconductors and the argumentation of the method is presented in Section IV. The discussion of the results is given in Section V. Finally, Section VI concludes this article.

II. Fabrication of the Films

Fabrication process of the superconducting NbTiN films has been previously studied in a number of papers [13], [14], [16], [18], [19], [20], and was described in brief by our group in [21]. There are many technological factors that contribute to the parameters of NbTiN films, e.g., substrate material and

Manuscript received 28 April 2023; revised 29 August 2023 and 18 September 2023; accepted 26 September 2023. Date of publication 2 October 2023; date of current version 3 November 2023. This work was supported by the Russian Science Foundation under Grant 23-79-00019 (https://rscf.ru/project/23-79-00019/) USU #352529 "Cryointegral" was used to fabricate the experimental samples in the framework of the State task at the Kotel'nikov IREE. USU was supported by the Ministry of Science and Higher Education of the Russian Federation under Grant 075-15- 2021-667. TDS measurements were performed within State Task of the Ministry of Science and Higher Education of the Russian Federation under Grant FSMG-2021-0005. *(Corresponding author: Fedor V. Khan.)*

Fedor V. Khan, Artem M. Chekushkin, and Valery P. Koshelets are with the Kotelnikov Institute of Radio Engineering and Electronics of RAS, 125009 Moscow, Russia (e-mail: khanfv@hitech.cplire.ru; chekushkin@hitech.cplire.ru; valery@hitech.cplire.ru).

Elena S. Zhukova, Boris P. Gorshunov, and Lenar S. Kadyrov are with the Moscow Institute of Physics and Technology, National Research University, 141701 Dolgoprudny, Russia (e-mail: zhukovaelenka@gmail.com; bpgorshunov@gmail.com; kadyrov.ls@mipt.ru).

Andrey V. Khudchenko is with the Astro Space Center of Lebedev Physical Institute of Russian Academy of Sciences, 119991 Moscow, Russia (e-mail: khudchenko@asc.rssi.ru).

Color versions of one or more figures in this article are available at https://doi.org/10.1109/TTHZ.2023.3321252.

Digital Object Identifier 10.1109/TTHZ.2023.3321252

TABLE I
DC PARAMETERS OF SUPERCONDUCTING NBTIN FILMS

	#1	#2	#3	#4	#5	#6
N_2 pressure, 10^{-3} mbar	0.65	0.59	0.53	0.47	0.41	0.35
Sputtering rate, Å/s	10.5	11.85	13.15	14.6	15.6	16.26
d, nm	333	332	328	339	338	325
$\sigma_{0,\,dc}$, 10^3 (Ω·cm)$^{-1}$	7.9	8.8	9.6	10.2	10.7	10.8
$T_{c,\,dc}$, K	14.9	15.2	15.2	15.3	15.2	14.8

temperature, presence of buffer layers, sputtering rate, and percentage of niobium, titanium, and nitrogen in the film. In [22], we investigated NbTiN films sputtered onto quartz and silicon substrates and found only minor difference between the parameters of the films. The lift-off process is often used in the fabrication of superconducting devices [21]. At temperatures above 150 °C, the photoresist baking occurs and lift-off process is no longer possible. This leaves little space for substrate temperature variation. The influence of the buffer layer will be studied elsewhere.

The samples in this article were sputtered on 535-μm thick high-resistivity silicon substrates at room temperature using Kurt J. Lesker cluster magnetron system. Sputtering was performed from a 3″ NbTi (78% wt. of Nb and 22% wt. of Ti) target of 99.95% purity in a mixture of nitrogen and argon. The distance between the target and the substrate (about 80 mm) was chosen to provide, on the one hand, good sputtering rate and, on the other hand, homogeneity over the substrate area. The power of the magnetron was around 500 W, which is the optimum for our setup. The initial pressure in the magnetron chamber was less than 10^{-8} mbar. The argon pressure remained at $5.6{\cdot}10^{-3}$ mbar for all the samples, while the pressure of nitrogen was varied from $0.35{\cdot}10^{-3}$ to $0.65{\cdot}10^{-3}$ mbar. The amount of nitrogen in the gas mixture plays a key role in the production process of NbTiN films as it affects not only the composition of the film, but also the sputtering rate. Therefore, it was selected as the parameter to optimize NbTiN films fabrication process in this article. The sputtering rate is less sensitive to changes of the total pressure in magnetron, but it largely determines the tension in the films. However, the analysis of tension in NbTiN films extends beyond the scope of this article and will be studied in future.

The values of critical temperature T_c and the normal state dc conductivity σ_0 just above the T_c, measured using four-probe technique for all the films are presented in Table I. The dc test samples were fabricated at the same technological run with the TDS samples. They have a form of a straight lines that are 10-mm long and 200-μm wide (50 squares). The setup allows to obtain results with an accuracy of 1%–2%.

III. MEASUREMENT TECHNIQUE

A. Description of TDS Principles

The study of the samples was conducted using the TeraView TPS Spectra 3000 commercial TDS. The choice of TDS as a measurement technique was driven by our previous experience

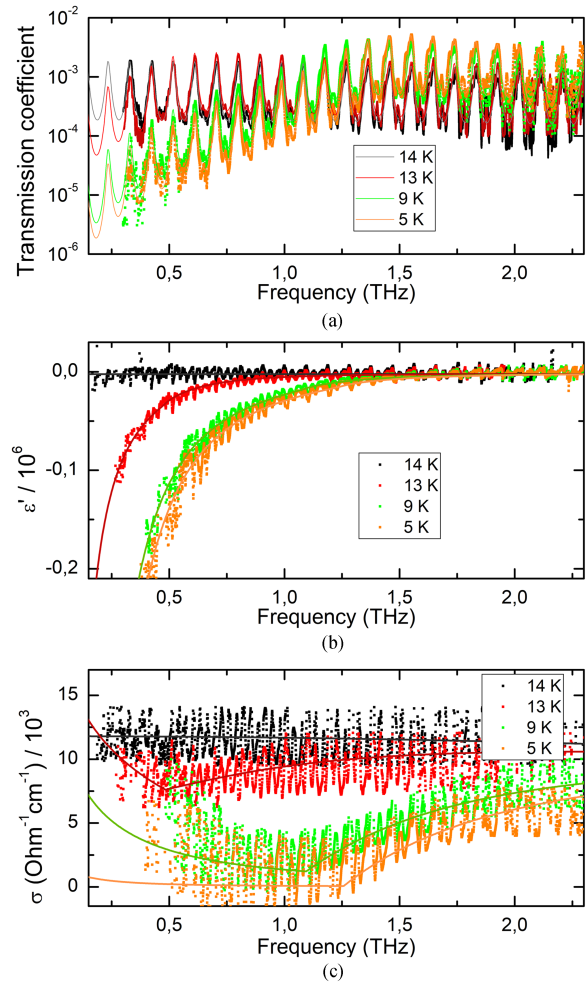

Fig. 1. Spectra of transmission coefficient *Tr* (a), real part of permittivity (b), and conductivity (c) of superconducting NbTiN film #5.

as TDS has a better signal-to-noise ratio when studying NbTiN films than DFTS [17]. The setup allows to measure complex transmission coefficient spectra of the superconducting films on substrates in frequency range up to 3 THz, which reliably covers the frequency interval where the superconducting gap frequency (≈1.2 THz) is located. THz radiation is generated and detected by semiconducting emitter and detector gated by ultra-short pulses of a Ti-sapphire laser. More than 10 spectra within a temperature range from 5 to 15 K were measured for each sample. The experimental transmission coefficient spectra of sample #5 at temperatures 5, 9, 13, and 14 K are shown in Fig. 1(a). The periodic structure of the transmissivity spectra is due to multiple reflections within the substrate.

The electrodynamic properties of the films both in normal and superconducting state can be described by complex permittivity $\varepsilon^* = \varepsilon' - 4\pi i\sigma_1/\omega$, where ε' is real part of permittivity, σ_1 is real part of conductivity, and ω is circular frequency. Spectra of ε' and σ_1 of the films were determined from the frequency-dependent complex transmission coefficient (both magnitude and phase). Spectra of electrodynamic response of the film on substrate were obtained by solving corresponding set of equations for two-layered medium [23]. Parameters of the substrate, including thickness, permittivity, and dielectric loss tangent, were extracted beforehand by studying the bare silicon plate with the same dimensions and without a film on its surface. Permittivity and conductivity spectra of the film #5 are depicted in Fig. 1(b) and (c), respectively. In the superconducting state, the permittivity sharply decreases as it approaches low frequencies. This can be described by the formula $\varepsilon' = -(\omega_{\mathrm{pl}}^{\mathrm{SC}}/\omega)^2$, where negative ε' values correspond to inductive response of Cooper pairs condensed under a zero-frequency delta-function in the conductivity spectrum. $\omega_{\mathrm{pl}}^{\mathrm{SC}}$ represents the plasma frequency of the superconducting condensate. Above the gap frequency $f_g = \omega_g/2\pi = 2\Delta/h$, the conductivity (absorption) is suppressed showing a kink around $2\Delta/h$ (h is Planck's constant) [24].

B. Theoretical Model

To model the conductivity and permittivity spectra and to determine the parameters of the superconducting films, we used the expressions from the work by Zimmermann et al. [25]. This model not only allows to calculate the frequency-dependent complex conductivity, but also takes into account finite quasi-particle scattering time, which enables to describe decline in the experimental conductivity curves at frequencies above the f_g. We express the scattering rate as $\gamma = \hbar/\tau$, where τ is quasiparticle scattering time.

Corresponding theoretical curves are shown by solid lines in Fig. 1. Transmission coefficient of the multilayer structure was calculated as discussed in [25]. The parameters Δ, γ, and σ_0 were obtained by fitting experimental data.

IV. Effects of Strong Coupling and Intragap States

In recent studies of NbN and NbTiN films [22], [26], the authors claim that it is necessary to take into account the intragap quasiparticle states in order to achieve good correspondence between theory and experiment at frequencies near the gap frequency. In corresponding models, it is assumed that for different reasons the singularity in density of states near the gap disappears and takes finite values, which can be handled by adding imaginary part to the gap [26], [27], [28]. More general way is to solve the Usadel equation [29], [30], which was done previously by a number of authors for Ti, Ti–Al layered systems, TiN, and NbTiN films [31], [32], [33]. In case of isotropic film with magnetic impurities, it can be explicitly shown that the model suggested by Nam [28] is a particular case of that described in the papers above [29], [30], [31], [32], [33].

Nb and its compounds are the superconductors with strong coupling. Because of the strong coupling, the BCS [24] expression $\Delta_0 = 1.76 k_B T_c$ is no longer valid (Δ_0 here is the gap value at $T = 0$ K, k_B is the Boltzmann constant). The relation between Δ_0 and T_c becomes more complex [34] and, in addition, depends on parameters λ and μ which denote the strength of electron–photon coupling and Coulomb pseudopotential, respectively. To our knowledge, the information on these parameters for NbTiN films in literature is absent. In [35], values of λ for Nb films obtained using different measurement techniques differ from each other and calculations within 10%. For these reasons, in present article, we simply use Δ_0 and T_c as independent fitting parameters. The coefficient at $k_B T_c$ was found to be larger than 1.76 (2.0–2.2 for all the NbTiN films measured in this article).

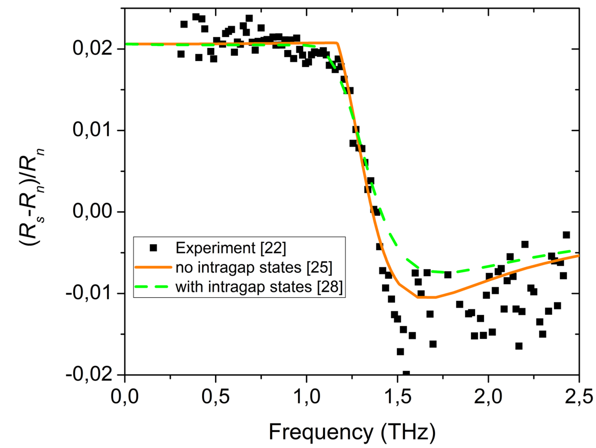

Fig. 2. Results for relative difference in reflection coefficients of NbTiN film in superconducting and normal state from [22]. Experimental data are shown by dots; dashed green and solid orange curves depict the theoretical results obtained with and without taking intragap states into account, respectively. The range below the gap with the biggest discrepancy between orange curve and experiment is marked with arrow.

As the model [25] describes the samples in the present article accurately enough, without making any assumptions on intragap states, it was intriguing to find out whether it could also be applied to the data measured by other groups.

In the article by Lap et al. [22], similar superconducting NbTiN films with the thicknesses exceeding London penetration depth are investigated. In that article, additional silicon plates were used in order to suppress multiple reflections within the substrate, and as a result only superconducting film sandwiched between vacuum and silicon media should be modeled. Theoretical curves together with the experimental data are shown in Fig. 2. The difference in reflection coefficients where film is in superconducting and normal states at low frequencies is fully determined by σ_0. By varying Δ, the position of the kink can be changed; the steepness of the kink can be adjusted by γ. Fitting was performed using least-square method with frequency points above 1.3 THz having smaller weight since at higher frequencies the accuracy of the measurements was limited by absorption in atmosphere. It can be seen that even without taking into account the intragap states the model still allows to fit the results of experiment with reasonable accuracy in the whole frequency range (see solid orange curve). The parameters of the fit were as follows: $T_c = 14.7$ K, $\Delta_0 = 2.4$ meV, $\sigma_0 = 8{\cdot}10^3$ $(\Omega{\cdot}\mathrm{cm})^{-1}$, and $\tau = \hbar/\gamma = 50$ fs.

However, small discrepancy occurs at frequencies 1–1.2 THz, i.e., near the gap frequency (1.16 THz), and especially below it (see the red arrow in Fig. 2). By utilizing the expressions from [28], this discrepancy can be resolved (dashed green curve in Fig. 2). The parameters σ_0 and γ remain the same as listed above in previous paragraph. The value of the parameter Γ_s that corresponds to scattering rate by magnetic impurities was $0.02{\cdot}\Delta_0$. This effect leads to broadening of the gap frequency ω_g feature, and also to a decrease of ω_g (2.1 meV compared to $\Delta_0 = 2.4$ meV when $\Gamma_s = 0$). Thus, Δ_0 was increased to

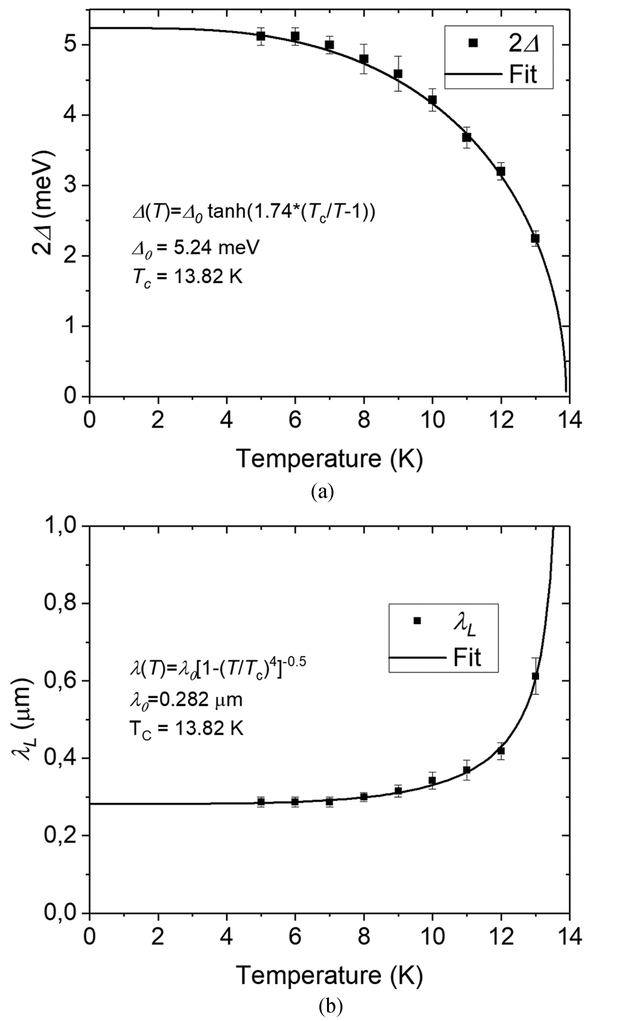

Fig. 3. Temperature dependences of superconducting gap parameter (a) and London penetration depth (b) of the sample #5. The data points were obtained from fitting the transmission spectra at corresponding temperature. Solid lines show least-square fits with (1) and (2), respectively.

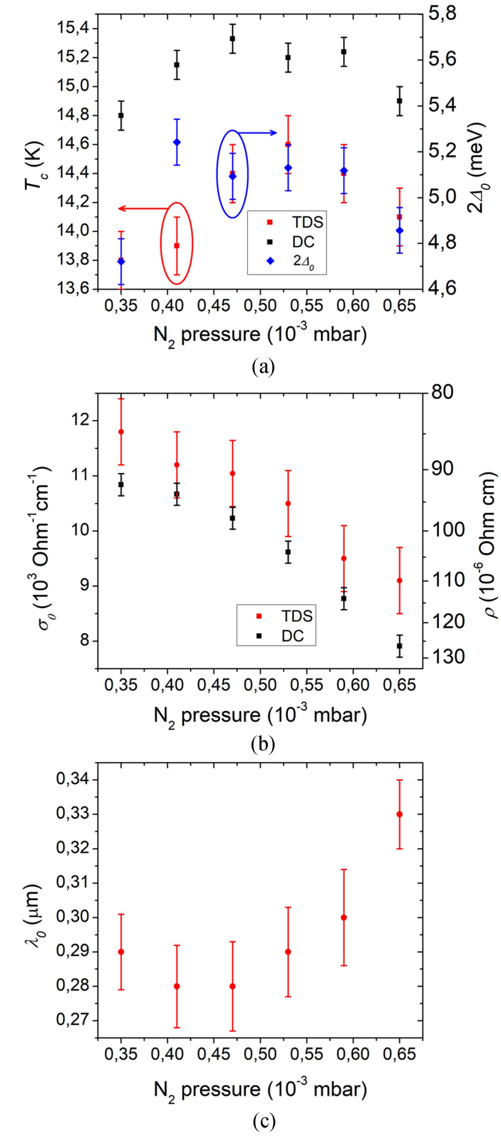

Fig. 4. Parameters of the NbTiN films fabricated at different pressures of nitrogen in magnetron chamber.

2.55 meV in order to obtain good agreement with experimental data at frequencies near 1.1 THz.

It still remains unclear whether decrease in reflectivity near the gap frequency is caused by intrinsic or extrinsic effects, such as surface roughness or contamination. What is more important, experiment and theory are in reasonable agreement for both models. Therefore, we assume that the aforementioned factors have a minor impact on the properties of thick NbTiN films and the model described in Section III-B is suitable for characterizing our films.

V. Results and Discussion

Temperature dependence of the superconducting gap $\Delta(T)$ is shown in Fig. 3(a). Each data point is obtained by fitting the corresponding spectra shown in Fig. 1(a). Solid line corresponds to empirical formula

$$\Delta\left(T\right) = \Delta_0 \; \tanh\left(1.74\sqrt{T_c/T \; - 1}\right) \qquad (1)$$

where Δ_0 is zero-temperature gap value.

We also present here data on London penetration depth since it significantly affects the phase velocity and, therefore, the propagation constant in superconducting transmission lines [36]. The procedure applied to determine the London penetration depth is the same as for Δ; data points at different temperatures are obtained from Fig. 1(b) [37]. Fitting the data points with the two-fluid model expression, presented as follows, allows to determine the zero-temperature value λ_0:

$$\lambda_L\left(T\right) = \lambda_0\sqrt{1-\left(\frac{T}{T_c}\right)^4}. \qquad (2)$$

Parameters σ_0 and γ were found to be constant at all temperatures for every individual film. This may be explained by the fact that the films were fabricated using magnetron sputtering, and therefore have crystalline structure resulting in quasiparticles mostly scatter by impurities. Moreover, γ was found to be nearly the same for all the films within the accuracy of the experiment. Corresponding scattering time τ was around 33 ns.

The resultant parameters of the films, namely, T_c, Δ_0, σ_0, and λ_0, measured both at dc and using TDS, depending on the pressure of nitrogen in magnetron, are shown in Fig. 4.

Difference between T_c values obtained from dc measurements and by analyzing the TDS data is likely caused by the grain structure of the films: at temperatures close to T_c, there are areas both in superconducting state and normal state. Direct current can flow through superconducting pattern and evade the areas that are in normal state, while the THz-radiation in TDS is more sensitive to material within superconducting grains. Therefore, significant increase of conductivity at THz frequencies will occur at lower temperatures where the film is in superconducting state, resulting in lower effective T_c.

Recently [38], the properties of superconducting NbTiN film were probed at dc and with the parallel plate resonator technique at frequency around 19 GHz and TDS. The T_c values obtained from TDS and resonator technique are the same within the accuracy of the experiments (13.1 and 13.3 K, respectively), while dc measurement yields 14.9 K which is in agreement with the present results. At the same time, the value of λ_0 determined with parallel plate resonator (230 nm) was found to be smaller than the one obtained from TDS (300 nm). We assume that the difference is caused by the frequency dependence of λ_L.

From Fig. 4, it can be seen that the critical temperature T_c of the films reaches its maximum value of 14.6 K at a nitrogen pressure around 0.55 10^{-3} mbar; the normal-state conductivity σ_0 decreases monotonously over the entire range under study and the London penetration depth λ_0 has a minimum value at 0.45 10^{-3} mbar [see Fig. 4(a), (b), and (c), respectively]. On the right axis of Fig. 4(b), the resistivity scale $\rho = 1/\sigma_0$ is plotted for convenience.

VI. Conclusion

To sum up, we performed a comprehensive study of THz electrodynamic properties of superconducting NbTiN films and determined the values of the nitrogen and argon pressure at which the films with the highest possible T_c, Δ_0, σ_0, and lowest λ_0 are obtained. The effects of the buffer layer and sputtering from the target with different Nb-Ti compound will be published elsewhere in the near future. It should be mentioned that there is a tradeoff between the parameters and the limit values are achieved at different manufacturing conditions. Furthermore, the TDS results deviate by approximately 10% from the dc measurement data. We argue that the difference is intrinsic to the films and therefore, it is the parameters obtained by TDS that should be used for modeling superconducting devices at high frequencies.

References

[1] W. E. Bron, "Spectroscopy of high-frequency phonons," *Rep. Prog. Phys.*, vol. 43, no. 3, pp. 301–352, 1980, doi: 10.1088/0034-4885/43/3/002.
[2] ALMA Observatory. 1999. [Online]. Available: https://almaobservatory.org/
[3] APEX Telescope. 2003. [Online]. Available: https://apex-telescope.org
[4] Millimetron Space Observatory. 2020. [Online]. Available: https://millimetron.ru
[5] Hershel Space Observatory. 2009. [Online]. Available: https://www.herschel.caltech.edu
[6] N. V. Kinev et al., "Terahertz spectroscopy of gas absorption using the superconducting flux-flow oscillator as an active source and the superconducting integrated receiver," *Sensors*, vol. 20, no. 24, Dec. 2020, Art. no. 7267, doi: 10.3390/s20247267.
[7] G. De Lange et al., "Development and characterization of the superconducting integrated receiver channel of the TELIS atmospheric sounder," *Supercond. Sci. Technol.*, vol. 23, no. 4, Mar. 2010, Art. no. 045016, doi: 10.1088/0953-2048/23/4/045016.
[8] K. A. Baksheeva et al., "The sub-THz emission of the human body under physiological stress," *IEEE Trans. Terahertz Sci. Technol.*, vol. 11, no. 4, pp. 381–388, Jul. 2021, doi: 10.1109/TTHZ.2021.3066099.
[9] C. M. Natarajan, M. G. Tanner, and R. H. Hadfield, "Superconducting nanowire single-photon detectors: Physics and applications," *Supercond. Sci. Technol.*, vol. 25, no. 6, Mar. 2012, Art. no. 063001, doi: 10.1088/0953-2048/25/6/063001.
[10] J. Aumentado, "Superconducting parametric amplifiers: The state of the art in Josephson parametric amplifiers," *IEEE Microw. Mag.*, vol. 21, no. 8, pp. 45–59, Aug. 2020, doi: 10.1109/MMM.2020.2993476.
[11] T. Kojima et al., "Three quanta sensitivity superconductor–insulator–superconductor mixer for the 0.78–0.95 THz band," *Appl. Phys. Exp.*, vol. 2, no. 10, Oct. 2009, Art. no. 102201, doi: 10.1143/APEX.2.102201.
[12] J. D. Garrett, B.-K. Tan, C. Chaumont, F. Boussaha, and G. Yassin, "A 230-GHz endfire SIS mixer with near quantum-limited performance," *IEEE Microw. Wireless Compon. Lett.*, vol. 32, no. 12, pp. 1435–1438, Dec. 2022, doi: 10.1109/LMWC.2022.3190701.
[13] Y. Uzawa et al., "Tuning circuit material for mass-produced terahertz SIS receivers," *IEEE Trans. Appl. Supercond.*, vol. 25, no. 3, Jun. 2015, Art. no. 2401005, doi: 10.1109/TASC.2014.2386211.
[14] Y. Uzawa et al., "Design of terahertz SIS mixers using Nb/AlN/Nb junctions integrated with All-NbTiN tuning circuits," *IEEE Trans. Appl. Supercond.*, vol. 27, no. 4, Jun. 2017, Art. no. 1500705, doi: 10.1109/TASC.2016.2632628.
[15] R. C. Taber, "A parallel plate resonator technique for microwave loss measurements on superconductors," *Rev. Sci. Instrum.*, vol. 61, no. 8, pp. 2200–2206, Aug. 1990, doi: 10.1063/1.1141389.
[16] L. Yu et al., "Fabrication of niobium titanium nitride thin films with high superconducting transition temperatures and short penetration lengths," *IEEE Trans. Appl. Supercond.*, vol. 15, no. 1, pp. 44–48, Mar. 2005, doi: 10.1109/TASC.2005.844126.
[17] A. Khudchenko et al., "Dispersive spectrometry at terahertz frequencies for probing the quality of NbTiN superconducting films," *IEEE Trans. Appl. Supercond.*, vol. 32, no. 4, Jun. 2022, Art. no. 1500506, doi: 10.1109/TASC.2022.3147736.
[18] A. Khudchenko et al., "High-Gap Nb-AlN-NbN SIS junctions for frequency band 790–950 GHz," *IEEE Trans. Terahertz Sci. Technol.*, vol. 6, no. 1, pp. 127–132, Jan. 2016, doi: 10.1109/TTHZ.2015.2504783.
[19] D. J. Thoen et al., "Superconducting NbTin thin films with highly uniform properties over a ∅ 100 mm Wafer," *IEEE Trans. Appl. Supercond.*, vol. 27, no. 4, Jun. 2017, Art. no. 1500505, doi: 10.1109/TASC.2016.2631948.
[20] B. G. C. Bos et al., "Reactive magnetron sputter deposition of superconducting niobium titanium nitride thin films with different target sizes," *IEEE Trans. Appl. Supercond.*, vol. 27, no. 4, Jun. 2017, Art. no. 1500405, doi: 10.1109/TASC.2016.2631939.
[21] A. M. Chekushkin et al., "Optimization of fabrication processes for Nb, NbN, NbTiN films and high-quality tunnel junctions for terahertz receiving circuits," *Tech. Phys.*, vol. 92, no. 13, pp. 2136–2140, Jul. 2022, doi: 10.21883/TP.2022.13.52234.135-21.
[22] B. N. R. Lap et al., "Characterization of superconducting NbTiN films using a dispersive Fourier transform spectrometer," *Appl. Phys. Lett.*, vol. 119, no. 15, Sep. 2021, Art. no. 152601, doi: 10.1063/5.0066371.
[23] M. Born and E. Wolf, *Principles of Optics*. Cambridge, U.K.: Cambridge Univ. Press, 1999, pp. 64–71.
[24] M. Tinkham, *Introduction to Superconductivity*. New York, NY, USA: McGraw-Hill, 1975, pp. 58–65.
[25] W. Zimmermann et al., "Optical conductivity of BCS superconductors with arbitrary purity," *Physica C: Supercond.*, vol. 181, no. 1, pp. 99–104, Nov. 1991, doi: 10.1016/0921-4534(91)90771-P.
[26] Y. Uzawa et al., "Optical and tunneling studies of energy gap in superconducting niobium nitride films," *J. Low Temp. Phys.*, vol. 199, pp. 143–148, Jan. 2020, doi: 10.1007/s10909-019-02324-1.

[27] T. Noguchi, M. Naruse, and Y. Sekimoto, "RF conductivity and surface impedance of a superconductor taking into account the complex superconducting gap energy," *Phys. Procedia*, vol. 36, pp. 318–323, Jun. 2012, doi: 10.1016/j.phpro.2012.06.166.

[28] S. B. Nam, "Theory of electromagnetic properties of superconducting and normal systems. I," *Phys. Rev.*, vol. 156, no. 2, pp. 470–486, Apr. 1967, doi: 10.1103/PhysRev.156.470.

[29] K. D. Usadel, "Generalized diffusion equation for superconducting alloys," *Phys. Rev. Lett.*, vol. 25, no. 8, pp. 507–509, Aug. 1970, doi: 10.1103/PhysRevLett.25.507.

[30] A. Anthore, P. Hugues, and D. Esteve, "Density of states in a superconductor carrying a supercurrent," *Phys. Rev. Lett.*, vol. 90, no. 12, Mar. 2003, Art. no. 127001, doi: 10.1103/PhysRevLett.90.127001.

[31] S. Zhao, S. Withington, D. J. Goldie, and C. N. Thomas, "Nonlinear properties of supercurrent-carrying single- and multi-layer thin-film superconductors," *J. Low Temp. Phys.*, vol. 199, no. 1/2, pp. 34–44, Jan. 2020, doi: 10.1007/s10909-019-02306-3.

[32] P. C. J. J. Coumou, E. F. C. Driessen, J. Bueno, C. Chapelier, and T. M. Klapwijk, "Electrodynamic response and local tunneling spectroscopy of strongly disordered superconducting TiN films," *Phys. Rev. B*, vol. 88, no. 18, Nov. 2013, Art. no. 180505, doi: 10.1103/PhysRevB.88.180505.

[33] E. F. C. Driessen, P. C. J. J. Coumou, R. R. Tromp, P. J. De Visser, and T. M. Klapwijk, "Strongly disordered TiN and NbTiN s-wave superconductors probed by microwave electrodynamics," *Phys. Rev. Lett.*, vol. 109, no. 10, Sep. 2012, Art. no. 107003, doi: 10.1103/PhysRevLett.109.107003.

[34] W. L. McMillan, "Transition temperature of strong-coupled superconductors," *Phys. Rev.*, vol. 167, no. 2, pp. 331–344, Mar. 1968, doi: 10.1103/PhysRev.167.331.

[35] R. Bauer, A. Schmid, P. Pavone, and D. Strauch, "Electron-phonon coupling in the metallic elements Al, Au, Na, and Nb: A first-principles study," *Phys. Rev. B*, vol. 57, no. 18, pp. 11276–11282, Dec. 1998, doi: 10.1103/PhysRevB.57.11276.

[36] R. L. Kautz, "Picosecond pulses on superconducting striplines," *J. Appl. Phys.*, vol. 49, no. 1, pp. 308–314, Aug. 1977, doi: 10.1063/1.324387.

[37] U. S. Pracht et al., "Electrodynamics of the Superconducting state in ultra-thin films at THz frequencies," *IEEE Trans. Terahertz Sci. Technol.*, vol. 3, no. 3, pp. 269–280, May 2013, doi: 10.1109/TTHZ.2013.2255047.

[38] F. V. Khan, "Characterization of superconducting NbTiN films using TDS, DFTS and parallel plate resonator," ISSTT-2022, Baeza, Spain, Rep. REG-194, Oct. 2022.

Fedor V. Khan received the B.S. and M.S. degree in applied mathematics and physics from the Moscow Institute of Physics and Technology, Dolgoprudny, Russia, in 2021 and 2023, respectively, where he is currently working towards his Ph.D. degree in condensed matter physics.

Since 2019, he has been an Engineer with the Kotelnikov Institute of Radio Engineering and Electronics of Russian Academy of Sciences, Moscow, Russia, working on characterization of the superconducting materials for THz-range electronics and modeling of superconducting devices.

Elena S. Zhukova received the M.S. degree in applied physics and mathematics and the Ph.D. degree in condensed matter physics from the Moscow Institute of Physics and Technology, Moscow, Russia, in 2007 and 2010, respectively.

From 2010 to 2014, she was a Junior Researcher with the A.M. Prokhorov General Physics Institute, Russian Academy of Sciences, Moscow, Russia. Since 2014, she has been a Senior Researcher and a Deputy Head of the Laboratory of Terahertz Spectroscopy, Moscow Institute of Physics and Technology (National Research Institute), Dolgoprudny, Russia. Her research interests include terahertz and infrared spectroscopy of systems with correlated electronic states.

Boris P. Gorshunov received the B.S. degree in physics from the Moscow Physical-Engineering Institute, Moscow, Russia, in 1978, and the Ph.D. degree in submillimeter spectroscopy of solids from the Russian Academy of Sciences, Moscow, Russia, in 1988.

He was with the Lebedev Physical Institute, Moscow, Russia, which is currently the A. M. Prokhorov General Physics Institute, Russian Academy of Sciences. He is currently leading the Laboratory of Terahertz Spectroscopy, Moscow Institute of Physics and Technology (National Research University). He spent many years abroad to work at universities in Regensburg, Los Angeles, Stuttgart, and other institutions. His research interests include the field of strongly correlated electronic phenomena in solids.

Lenar S. Kadyrov received the B.S. and M.S. degree in applied mathematics and physics from the Moscow Institute of Physics and Technology, Dolgoprudny, Russia, in 2011 and 2013, respectively, and the Ph.D. degree in physics from the Moscow Institute of Physics and Technology, in 2016, for his work on infrared/terahertz spectroscopy of charge-ordered manganites.

He was working as a Junior Researcher with the A. M. Prokhorov General Physics Institute of Russian Academy of Sciences, in the period 2013–2016. Starting with 2016, he is currently working as a Researcher with the Moscow Institute of Physics and Technology. His research interests include the field of terahertz-infrared spectroscopy of condensed matter and scientific software development.

Artem M. Chekushkin, photograph and biography not available at the time of publication.

Andrey V. Khudchenko received the M.S. degree in applied physics and mathematics and the Ph.D. degree in radio physics from the Moscow Institute of Physics and Technology, Moscow, Russia, in 2007 and 2009, respectively.

Since 2009, he has been a Researcher with the Kotel'nikov Institute of Radio Engineering and Electronics, Moscow, Russia. From 2009 to 2015, he was an Instrument Scientist with The Netherlands Institute for Space Research SRON, Leiden, The Netherlands, and from 2015 to 2020, an Instrument Scientist with the Kapteyn Astronomical Institute, University of Groningen, Groningen, The Netherlands. Since 2020, he joined the Astro Space Center of Lebedev Physical Institute. The main activity is related to the development of new heterodyne THz instruments.

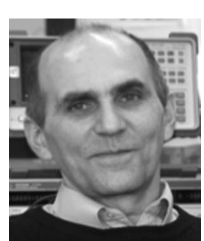

Valery P. Koshelets (Member, IEEE) received the M.S. degree in physics from the Lomonosov Moscow State University, Moscow, Russia, in 1973, and the Ph.D. degree in radio physics and the D.Sc. (Habilitation) degree in physical electronics from the Kotel'nikov Institute of Radio Engineering and Electronics of the Russian Academy of Sciences, Moscow, Russia, in 1978 and 1990, respectively.

Since 1973, he has been with the Kotel'nikov Institute of Radio Engineering and Electronics, Russian Academy of Sciences, Moscow, Russia, where he is currently the Head of the Laboratory of Superconducting Devices for Signal Detection and Processing.